

## **Automatic tracking of the life cycle of contrails**

M. Vázquez-Navarro, H. Mannstein, B. Mayer  
Institut für Physik der Atmosphäre, Deutsches Zentrum für Luft- und Raumfahrt,  
DLR Oberpfaffenhofen, Germany  
[Margarita.Vazquez@dlr.de](mailto:Margarita.Vazquez@dlr.de), [Hermann.Mannstein@dlr.de](mailto:Hermann.Mannstein@dlr.de),  
[Bernhard.Mayer@dlr.de](mailto:Bernhard.Mayer@dlr.de)

**Abstract:** The aim of this work is to describe an automatic tracking algorithm that allows the study the life cycle of contrails and their evolution to contrail cirrus in order to understand and quantify their influence on climate. First, a Rapid Retrieval of broadband fluxes based on MSG/SEVIRI is described and validated. The advantage of the method is its very high spatial and temporal resolution. Secondly, a MSG/SEVIRI based automatic tracking algorithm is presented. This algorithm provides a contrail binary mask that allows the study of the contrail physical properties throughout its lifetime.

**Keywords:** Contrail, contrail tracking, radiative forcing, MSG/SEVIRI

### **1 Introduction**

Aircraft operations can give rise to anthropogenic clouds called condensation trails (contrails) that under appropriate atmospheric conditions can spread out and eventually cover large areas in the upper troposphere. Since contrails consist of ice, the resulting clouds are termed contrail cirrus. Fresh contrails are easily detectable by their linear shape. Contrail cirrus are naturally looking cirrus but would not exist without prior formation of a linear contrail. The IPCC special report on aviation and the Global Atmosphere attributed the second largest warming climate effect (in terms of radiative forcing) of aviation specific emissions to linear contrails. The contribution of contrail cirrus was estimated to be even larger, but still very uncertain. To improve contrail detection and tracking and to combine information from polar orbiting satellites (high spatial resolution) and Meteosat Second Generation –MSG- (high temporal resolution) helps to study the effect that aircraft traffic has on cloud formation and therefore on climate.

The impact of contrails on climate through the radiation budget depends on their coverage and radiative properties. The interaction of a cloud with radiation depends on its microphysical properties (e.g. cloud phase, droplet or particle size and shape, water or ice content). Satellite data is ideal for studying cloud occurrence because of the regular availability for large areas. In this work, the Spinning Enhanced Visible and Infrared Imager (SEVIRI) on the European geostationary platform Meteosat Second Generation (MSG), is used to determine a number of physical properties of contrails and contrail cirrus such as cloud phase, cloud optical thickness, cloud particle size, cloud morphology and to improve the existing knowledge on their influence on the radiation budget.

Before undertaking a statistical approach, several case studies have been used as "test cases". Those contrails have been carefully observed and a number of properties have been studied (optical thickness through different methods, outgoing long- and shortwave radiative flux density, brightness temperature, spreading ratio).

## **2 Retrieval of broadband radiation fluxes from MSG/SEVIRI**

Any energy exchange between the Earth and the rest of the universe takes place through radiative transfer. We can consider the sun as the only source of energy for the Earth. The Earth atmosphere system reflects and absorbs solar radiation and re-emits it back into the space according to its temperature.

The presence of clouds modifies this emission. The cirrus-like clouds radiate back to the space at the lowest temperatures. Remote sensing of top of atmosphere broadband fluxes can help to accurately quantify the contribution of air traffic to the rising of this type of clouds.

In the study of the influence of small scale features in the atmosphere, the retrieval of broadband fluxes is necessary in a high temporal and spatial resolution. The usual broadband instruments offer a coverage that is useful in climate studies but, for instance, rapid changing features such as contrails are often ignored. The instruments on board of MSG offer a high temporal resolution (15 minutes in full-scan, 5 minutes in rapid-scan mode) and, thanks to the HRV channel, a very high spatial resolution (1 km x 1 km at the sub-satellite point), thus a Rapid Retrieval of broadband fluxes from MSG/SEVIRI offers a new tool for the study of small-scale features of the atmosphere. The Rapid Retrieval of Broadband Fluxes has been validated with reliable tools such as CERES (onboard TERRA/AQUA/TRMM) and the Geostationary Earth Radiation Budget experiment (GERB, onboard of the MSG satellites).

Accurate top-of-atmosphere (TOA) broadband fluxes are necessary for the study cloud radiative effects on the Earth-atmosphere system. Spectral broad-band radiometers on a geostationary platform provide measurements of radiation budget parameters within time frames of less than an hour, and global coverage, will provide the scientific community with a unique dataset that will enhance our understanding of climate.

In the study of the effects of cloudiness in the radiative system, very high absolute accuracy and long-term stability are required: one of the most important features of clouds is that they are constantly changing: horizontally, vertically, and in time. This difficult their study and requires a very high temporal resolution (an advantage of geostationary tools) and very high spatial resolution (to be found at polar orbiting satellites).

The motivation of using SEVIRI based narrowband-to-broadband conversion instead of the GERB provided broadband fluxes, is twofold:

- The need for higher spatial resolution for some applications (e.g. environmental impact of air traffic).
- The need of a very fast algorithm to process data for longer time periods (for reprocessing need not only near-real time but much faster).

The method used is based on a large set of forward simulations; is applied to MSG/SEVIRI and validated with MSG/GERB and TERRA/CERES.

The geostationary satellite Meteosat Second Generation (MSG) [9] is the operational European geostationary weather satellite. The two instruments on board of MSG used in this study are: the Spinning Enhanced Visible and Infra-Red Imager (SEVIRI) and the Geostationary Earth Radiation Budget (GERB).

#### *SEVIRI*

The Spinning Enhanced Visible and Infra-Red Imager (SEVIRI) is the radiometer onboard the geostationary satellite Meteosat Second Generation (MSG) [9]. MSG/SEVIRI became operational at the end of January 2004, provides data with a high temporal resolution of 15 minutes (5 minutes in the rapid scan mode, operational in June 2008). SEVIRI comprises twelve spectral bands: four solar, seven thermal infrared, and a combined solar/thermal channel at  $3.9\mu\text{m}$ . The spatial resolution is  $3\text{ km} \times 3\text{ km}$  at the sub-satellite point, except for the broadband high-resolution visible (HRVIS) channel which has resolution of  $1\text{ km} \times 1\text{ km}$  at the sub-satellite point.

#### *GERB*

GERB (Geostationary Earth Radiation Budget) is the broadband radiometer onboard MSG. It has two channels:  $0.32 - 4.0\ \mu\text{m}$ , with quartz filter and  $0.32 - 30\ \mu\text{m}$  without filter and by subtraction:  $4.0\ \mu\text{m} - 30\ \mu\text{m}$ . Spatial GERB resolution is very low, half a degree:  $44.6 \times 39.3\text{ km}$  (NS x EW) at nadir, although the temporal is very good: full earth disc, both channels in 5 minutes.

The radiance to flux conversion for each pixel is given by the cloud cover and the type of surface detected by SEVIRI. There are 24 lookup tables that provide information about the cloud phase and the optical thickness for six different types of surface. Besides, a cloud mask in SEVIRI spatial resolution is used. The flux is then estimated from radiance using Angular Dependency Models [2].

GERB has been validated using CERES radiometers, described below.

#### *CERES*

Clouds and the Earth's Radiant Energy System (CERES) is a system designed to provide a dataset of climate data useful for the study of the influence of clouds in the radiative budget. It is on board three satellites TERRA, AQUA and TRMM. CERES combines narrowband sensors to retrieve data about clouds and broadband sensors to retrieve radiative fluxes in short and longwave on the surface and at TOA. CERES validation is described in [1].

The ADMs needed to retrieve the fluxes are thoroughly described in [5] and their validation in [4].

The channels are shortwave (0.2 - 5  $\mu\text{m}$ ) and broad spectrum (0.2 – 100  $\mu\text{m}$ ), longwave broadband radiation is obtained by subtraction (0.5-100  $\mu\text{m}$ ). Besides, the window channel 8-12  $\mu\text{m}$  is included to improve the flux estimates. CERES/TERRA spatial resolution is 20 to 50 km in cross-track scan and temporal is twice a day.

For this work, images with three different spatial resolutions are used, depending on the instrument used. For homogeneity reasons, MSG/CERES and TERRA/GERB images will be mapped on the MSG/SEVIRI grid.

#### *Forward Model Data Set*

To establish the relationship between MSG/SEVIRI radiances and broadband fluxes, a huge set of forward calculations of the 11 MSG/SEVIRI channels (excluding the high-resolution visible channel, HRV) plus the corresponding reflected solar and outgoing thermal irradiances was done with the radiative transfer package libRadtran [8].

Reflectivities for the solar and equivalent brightness temperatures for the thermal SEVIRI channels have been simulated for different atmospheric and surface conditions. libRadtran offers a flexible interface to setup the atmospheric and surface conditions as well as a choice of different radiative transfer equation solvers. libRadtran has been successfully validated in several model intercomparison campaigns and by direct comparison with observations, for instance [7] and [11].

The libRadtran dataset used includes 10000 different combinations of atmospheric conditions as input (pressure, temperature, water vapour, ozone concentration, ice cloud optical thickness, ice particle effective radius, multilayer clouds...). For each combination of parameters, brightness temperatures were calculated for satellite zenith angles between 0° and 78°.

The broadband flux retrieval used in this work is thoroughly described in [3]. To perform the narrowband to broadband conversion in the SW region, a neural network is needed. libRadtran package was used to retrieve the following magnitudes to train the neural network and obtain SW radiative flux density: radiance VIS006, Radiance VIS008, radiance IR\_016, satellite zenith angle, solar zenith angle, relative azimuth, land/sea mask.

LW radiative flux density is retrieved using MSG/SEVIRI brightness temperatures according to a multilinear parameterisation given by equation (1):

$$F_{LW}^{\uparrow}(\Theta_{sat}) = \sigma \left\{ a(\theta_{sat})T_{6.2} + b(\theta_{sat})T_{7.3} + c(\theta_{sat})T_{8.7} + d(\theta_{sat})T_{9.7} + e(\theta_{sat})T_{10.8} + f(\theta_{sat})T_{12.0} + g(\theta_{sat})T_{13.4} + h(\theta_{sat}) \right\}^4 \quad (1)$$

where  $T_n$  is the brightness temperature of channel n  
 $\theta_{sat}$  is the satellite zenith angle  
 $a \dots h$  are fit constants.

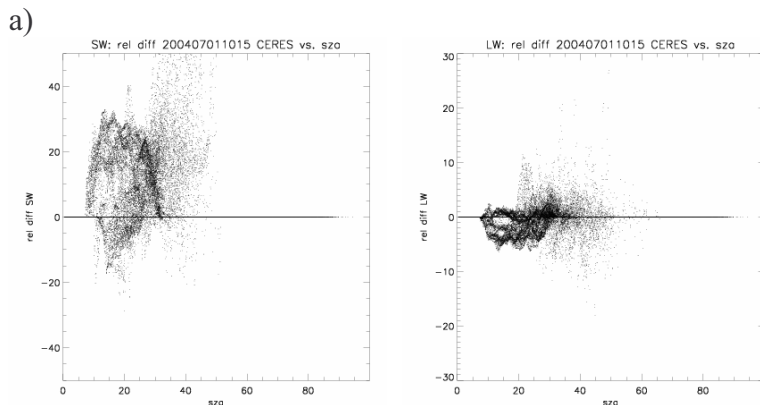
### Validation

Comparisons of CERES measured radiative flux densities (LW and SW) and their retrieved counterpart from MSG/SEVIRI algorithms were analysed (table 1). Processing of the images includes mapping of both data on the same grid.

Instrument		LW		SW	
MSG	CERES	R2	Slope	R2	Slope
01/02/04 08:30	08:23 – 08:38	95.24	0.94	94.60	0.97
02/02/04 02:15	02:07 – 02:23	90.44	0.89	-	-
24/03/04 08:00	08:00 – 08:13	94.06	0.96	87.97	0.87
08/04/04 07:30	07:14 – 07:29	95.01	0.97	91.82	0.87
14/06/04 11:15	09:02 – 09:21	95.15	1.00	93.20	0.80
01/07/04 08:30	08:16 – 08:35	94.53	0.99	87.87	0.76
01/07/04 11:45	11:31 – 11:50	94.56	0.94	93.15	0.80
01/07/04 12:00	12:00 – 12:08	99.02	0.98	96.09	0.83
08/07/04 12:00	12:00 – 12:08	99.02	0.98	96.09	0.83
13/08/04 14:45	14:39 – 14:59	87.34	0.87	87.62	0.81
02/09/04 12:45	12:38 – 12:57	92.46	0.93	92.49	0.84
15/10/04 18:45	18:35 – 18:59	88.86	0.91	-	-
10/11/04 21:00	20:50 – 20:59	88.48	0.95	-	-
22/12/04 02:15	02:07 – 02:23	96.40	1.00	-	-

Table 1: Comparison MSG/SEVIRI vs. CERES outgoing LW and SW radiative flux densities.

The comparisons were good but not perfect, neither in the SW nor in LW regions, so possible causes of discrepancies were analysed by plotting relative differences between CERES and MSG/SEVIRI fluxes as a function of solar zenith angle (Fig. 1a), satellite zenith angle (Fig. 1b), time delay between TERRA and MSG overpasses (Fig. 1c), latitude (Fig. 1d), cloud cover for all cloud types (Fig. 1e), and cirrus cover (Fig. 1f).



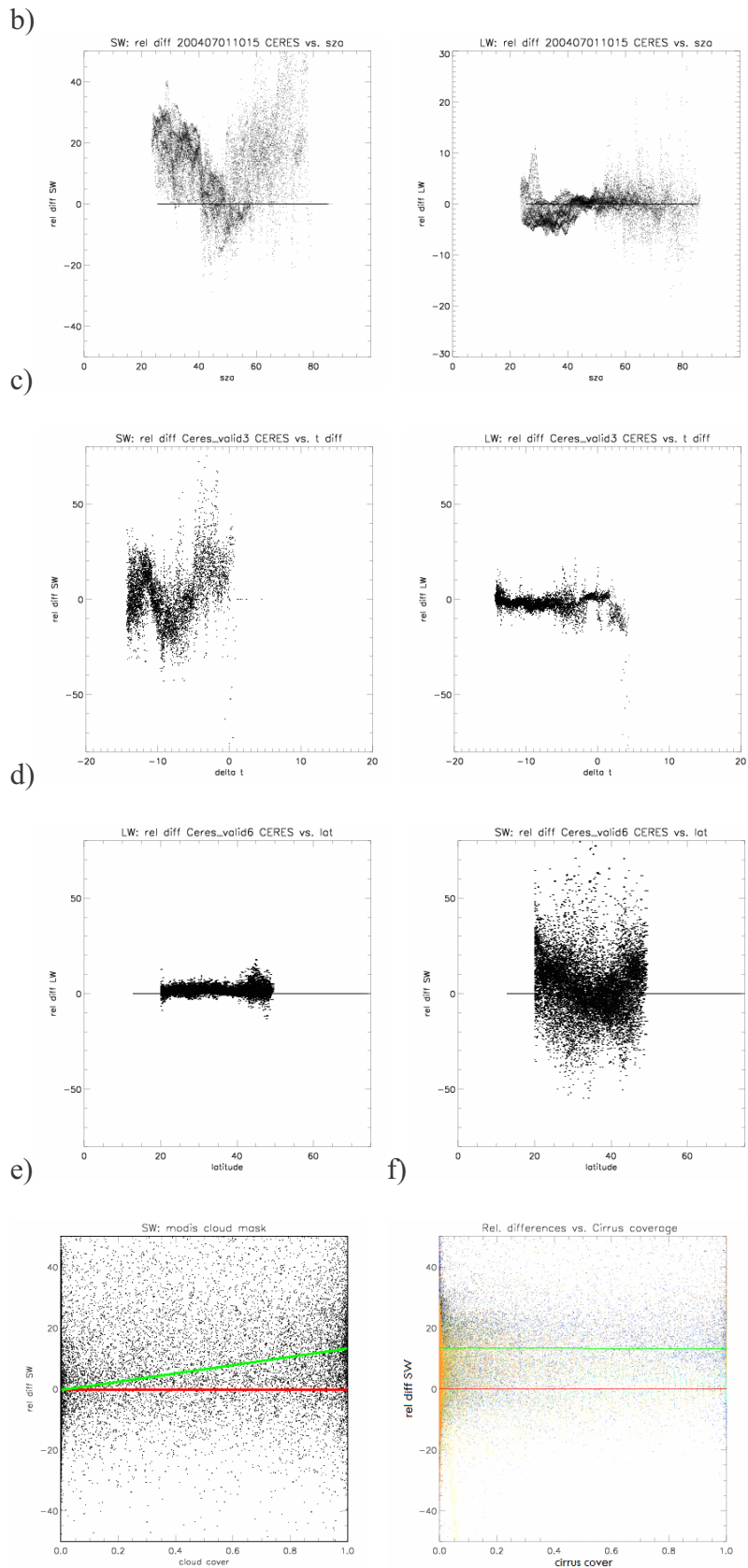


Fig. 1. Relative differences MSG/SEVIRI vs GERB vs. a) solar zenith angle, b) satellite zenith angle, c) time delay between overpasses, d) latitude, e) cloud cover -all cloud types-, f) and cirrus cover, for some of the scenes studied. Only e) shows an increase of the relative differences.

A similar analysis was carried on with the GERB instrument, with whom SEVIRI shares the viewing geometry. The improvement of the results was clear (table 2)

	Instrument		LW		SW	
	MSG	GERB	R2 (%)	Slope	R2(%)	Slope
12/05/06 20:00	19:59	99.81	0.99	97.82	1.40	
12/05/06 19:45	19:42	99.80	0.99	98.19	1.39	
15/05/06 18:30	18:39	99.65	0.99	97.92	1.14	
18/05/06 11:30	11:27	99.70	1.00	98.56	0.97	
20/05/06 03:00	03:00	99.66	0.98	-	-	
22/05/06 00:15	00:14	99.65	0.98	-	-	
25/05/06 15:00	15:01	99.70	0.99	97.93	0.99	
29/05/06 14:15	14:17	99.66	1.00	97.84	0.96	
01/06/06 12:45	12:41	99.64	1.00	97.92	0.95	
03/06/06 10:00	09:54	99.76	1.00	98.06	0.96	
10/06/06 22:00	22:02	99.60	0.99	-	-	
12/06/06 07:30	07:24	99.67	0.99	98.41	0.94	

Table 2: Comparison MSG/SEVIRI vs. GERB outgoing SW and LW radiative flux densities.

*CERES- MSG/SEVIRI:* retrieved flux density discrepancies independent of cirrus cover, latitude, time delay between satellite overpasses, and sun/sat geometry but dependent of cloud cover.

*GERB - MSG/SEVIRI:* significant improvement in correlation due to the fact that both instruments are onboard a geostationary satellite and share the same view of the Earth. The 3-dimensional structure of clouds affects both sensors in the same way and therefore explains the discrepancies in the previous case.

Thus, both MSG/SEVIRI based algorithms are validated and can be used as a tool to retrieve radiative flux density with the temporal and spatial resolution of the SEVIRI sensor.

### 3 Automatic Tracking Algorithm

A contrail detection algorithm based on a combination of spectral information, image segmentation and object classification runs on a polar orbiting satellite (e.g. MODIS). Due to the high spatial resolution, the detection algorithm combines a relatively high detection efficiency with a low false alarm rate for linear contrails. Within the data of geostationary satellites, the identification of contrails is limited by the lower spatial resolution, but once they are identified, they can be tracked with time steps down to 5 minutes. Therefore automatically detected contrails from high resolution data of polar orbiting satellites are mapped onto the low resolution data of METEOSAT-8. Taking advantage of the rapid scan mode (temporal resolution: 5 minutes), they are tracked from the initial position back to the moment when they first arise and forth until eventually they are no longer distinguishable from the background (Fig 2).

The automatic tracking algorithm works in two steps. The goal of the first step is to define a line that will identify the contrail and the second step identifies, with the help of the line, the pixels that belong to the contrail. The input of the algorithm is a contrail detected in a MODIS data set, this is then mapped on Meteosat-9. The algorithm looks for a new line to define the same contrail in the following/previous timeslot ( $\Delta t=5$  minutes) selecting some "guide pixels" according to the following criteria:

- the brightness temperature difference  $12 \mu m - 11 \mu m$  must be lower than 2K,
- the pixels must be very distinguishable from the background (image processing),
- the new position has to be consistent with the wind field.

In case the criteria are not fulfilled or the resulting guide pixels are only two, a new set of similar criteria but with stronger thresholds is applied to eliminate any misidentification of neighbouring cloudy pixels and to force the identification of the contrail.

Once each timeslot has a line defined that identifies the contrail, new criteria are applied to select only contrail pixels, involving:

- the brightness temperature of the water vapour channel  $6.5 \mu m$ ,
- the brightness temperature difference of channels  $12 \mu m$  and  $11 \mu m$ ,
- image processing involving feature enhancement and edge detection algorithms

These criteria are applied to the pixels in the surrounding of the line in a fuzzy logic scheme. Possible pixels are given different probabilities of being contrail and only the most probable ones are labelled as contrail pixels. The whole process is then iterated until it arrives to the arising or eventual vanish of the contrail as depicted in Fig. 2.

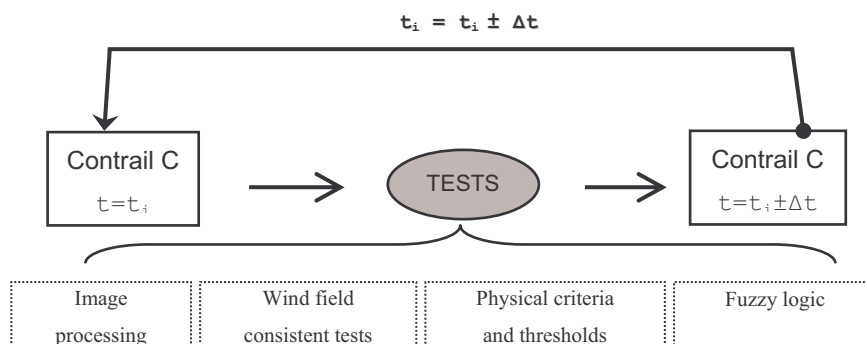


Fig. 2: *Contrail tracking algorithm.*

The resulting binary mask can then be used to retrieve different physical and geometrical properties of the contrail such as brightness temperature, radiative flux density using the above mentioned algorithms, optical thickness, area, lifespan... and eventually radiative forcing.

For the time being, the algorithm combines MODIS with SEVIRI, but other polar orbiting platforms such as the AVHRR onboard the NOAA satellites and MetOp could be used as well to identify the starting lines in the SEVIRI data. Results (Fig. 3) show that the algorithm works well, tracks a contrail even in scenes with many other contrails nearby or crossing, and furthermore, when a contrail has lost most of its linearity and splits in smaller parts. In the case depicted in Fig 3. the MODIS detected contrail, i.e. the algorithm initial point was at 1150UTC. The advantage of the algorithm is that it considers the whole life cycle of a contrail, which is a task that common linear contrail detection algorithms can not fulfil.

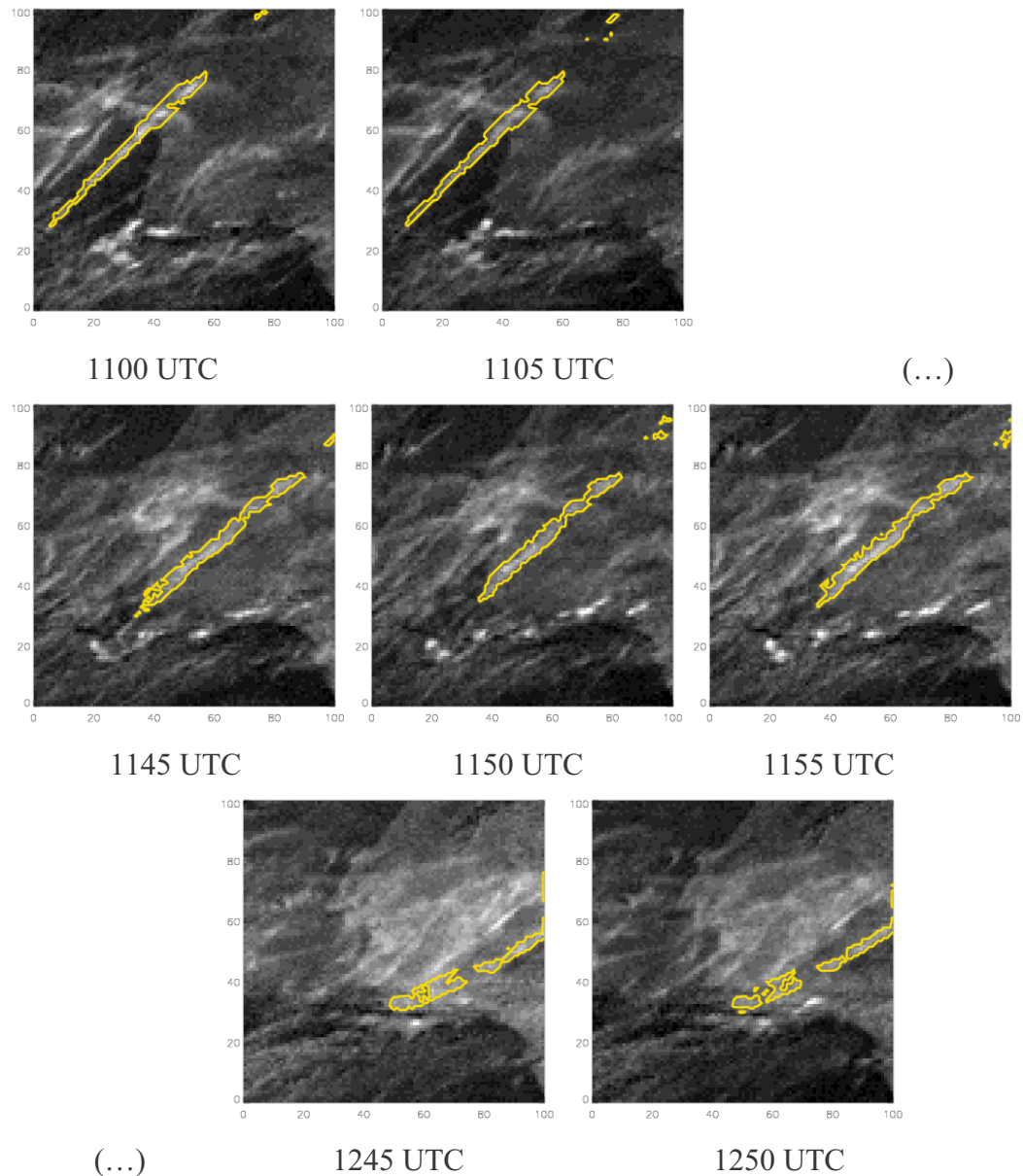


Fig 3. Some stages of the evolution of a contrail over the south of Portugal on the 3<sup>rd</sup> June 2008 tracked with the Automatic Contrail Tracking Algorithm.

Some of the physical properties that can be retrieved thanks to the mask provided by the algorithm are shown below. Fig. 4 shows the evolution of the outgoing flux density in SW and LW retrieved with the algorithm mentioned in section 2 and the evolution of the optical thickness retrieved with a neural network based algorithm. It can be seen that whereas the LW outgoing radiative flux density and

thus, the temperature, remain mostly constant, the SW outgoing radiative flux density and the optical thickness strongly decrease, because the contrail is spreading and becoming less visible. In addition, geometrical properties (area, spreading ratio) and radiative forcing (comparing the outgoing flux density of the contrail with that of its surroundings) can also be retrieved.

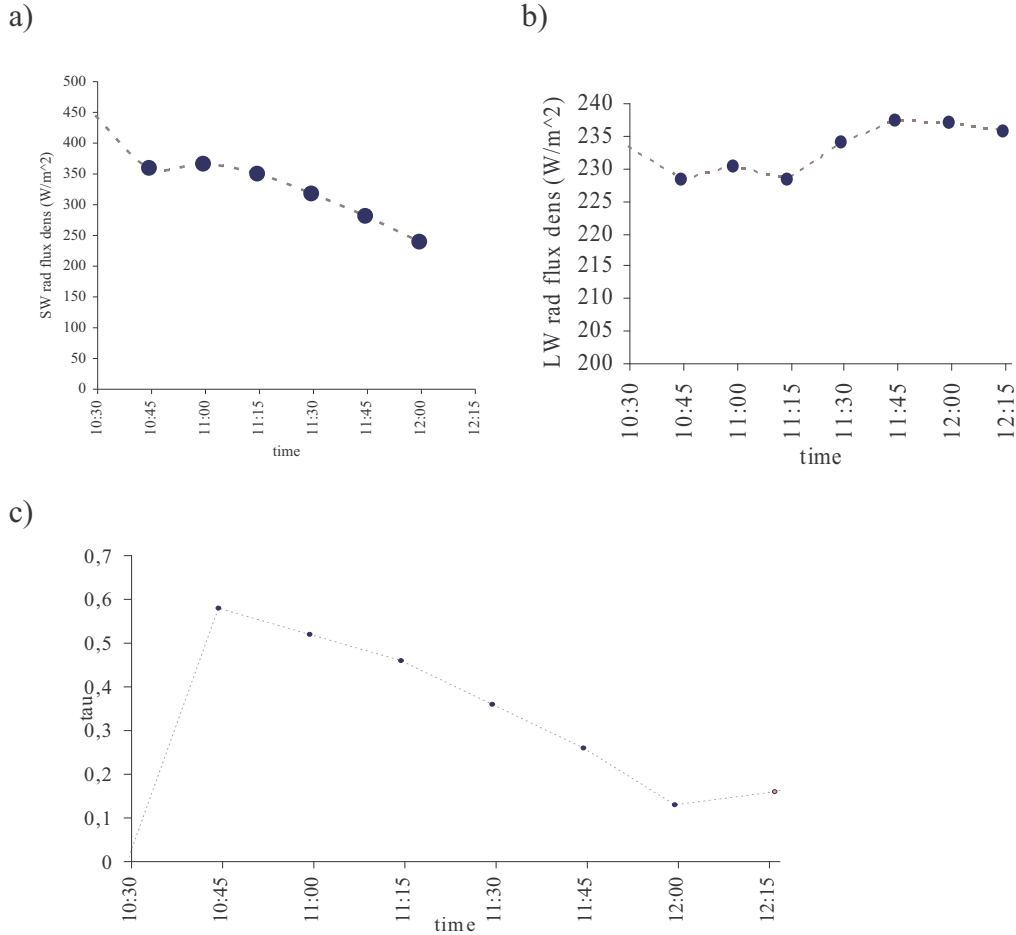


Fig. 4. Evolution of a) SW outgoing radiative flux density of a contrail, b) LW outgoing radiative flux density of a contrail, c) optical thickness.

#### 4 Conclusions

An automatic tracking algorithm especially designed for contrail tracking has been developed. It takes into account not only geometrical properties of contrails, but also physical properties, which allows the tracking of contrails when those loose linearity and are spread in small fragments.

The mask produced by the algorithm is used to assess physical properties of the contrail pixels such as lifespan, spread ratio, optical thickness, outgoing radiative flux density in the LW and SW regions and, eventually, the radiative forcing of contrails.

## 5 References

- [1] Charlock, T. P. y T. L. Alberta (1996). *The CERES/ARM/GEWEX Experiment (CAGEX) for the Retrieval of Radiative Fluxes with Satellite Data*. Bull. American Met. Soc. (77)11:2673-2683
- [2] Harries, J. E. et al., 2005. *The Geostationary Earth Radiation Budget Project*. Bull. American Met. Soc. (86)7:945 – 960
- [3] Krebs, W. et al., 2007, *Technical note: A new day- and night-time Meteosat Second Generation Cirrus Detection algorithm MeCiDA*, ACP, 7, 6145-6159
- [4] Loeb, N. G. et al., 2003, *Angular Distribution Models for Top-of-Atmosphere radiative flux estimation from the Clouds and the Earth's Radiant Energy System instrument on the Tropical Rainfall Measuring Mission Satellite. Part II. Validation*. Journal of App. Meteor. (42)1748-1769
- [5] Loeb, N. G., Kato, S., 2005. *Angular Distribution Models for Top-of-Atmosphere radiative flux estimation from the Clouds and the Earth's Radiant Energy System instrument on the TERRA satellite. Part I. Methodology*. Journal of Atm. and Oceanic Technology 22:338-351
- [6] Mannstein, H. et al. 1999, *Operational detection of contrails from NOAA-AVHRR-data*, Int. J. Remote Sensing, 20(8):1641–1660.
- [7] Mayer, B., et al., 1997, *Systematic long-term comparison of spectral UV measurements and UVSPEC modelling results*. Journal of Geophysical Research, 102(D7):8755-8767, 1997.
- [8] Mayer, B., A. Kylling, 2005, *Technical Note: The libRadtran software package for radiative transfer calculations: Description and examples of use*. Atmos. Chem. Phys. Discuss., 5:1319–1381.
- [9] Schmetz, J., et al., 2002, *An Introduction to Meteosat Second Generation (MSG)*. Bulletin of the American Meteorological Society, 83:977–992.
- [10] Schumann, U., 1996; *On conditions for contrail formation from aircraft exhausts*, Meteorologische Zeitschrift, 5:4–23.
- [11] Van Weele, M. et al., 2000, *From model intercomparisons towards benchmark UV spectra for six real atmospheric cases*. Journal of Geophysical Research, 105(D4):4915-4925, 2000.